BEHAVIOUR OF ELECTRON BEAM IN COMBINED A SELF-GENERATED FIELD AND A REVERSED GUIDE FIELD IN THE HELICAL WIGGLER

Soon-Kwon Nam * and Ki-Bum Kim

Department of Physics, Kangwon National University, Chunchon 200-701, Republic of Korea

Abstract

We have studied behaviour of electron beam in combined a self-generated field and a reversed axial-guide field in the tapered helical wiggler. The divergence of electron beam is caused by three-dimensional effects on the electron beam loss, we employ a tapered and reversed axial-guide field magnetic field. Evolution of energy spread and emittance of electron beam are investigated using three dimensional simulation. Beam cross-section, transverse momentum variation and cross-section view of electron beam are also calculated along z axis. The electron beam loss is reduced by optimizing the magnetic field strength and tapering parameter of reversed axial guide field.

INTRODUCTION

In free-electron laser(FEL), the gain increases when the beam current and the wiggler field amplitude are increased. When the free-electron laser experiments operate at the high-current regime and the intense wiggler field regime to get the sufficiently large gain, the axial-guide field make us to steer the electron beam in the axial direction [1–4] and the electron motion can be altered by the axial-guide field and self-field effects [5–11] .

In this work, we study the behaviour of electron beam in combined a self-generated field and a reversed axial-guide field in the tapered helical wiggler. Cross-section, profile and density of electron beam are investigated using three dimensional simulation.

THE SELF-GENERATED FIELD AND EXTERNAL FIELD

The space charge and current of electron beam generate the self-electric and self-magnetic fields. The Maxwell's equations in steady state are

$$\nabla \cdot \mathbf{E} = 4\pi\rho_0 \ , \ \nabla \times \mathbf{B} = \frac{4\pi}{c}\mathbf{J} \tag{1}$$

We assume that equilibrium properties (electron density and velocity) are uniform in the z-direction with $\partial n_b/\partial z = 0$ and $\partial v_b/\partial z = 0$. There is no equilibrium electric field parallel to z-direction with $\mathbf{E} \cdot \hat{e}_z = 0$. Where n_b is electron density and v_b is mean velocity of electron. The radial density and velocity profiles are assumed to be azimuthally

* snam@kangwon.ac.kr; Tel:+82-33-250-8463; fax:+82-33-257-9689

symmetric about the z-axis. Therefore the density and velocity profiles can be written as only function of r, that is,

$$n_b(r, \theta, z) = n_b(r), \ v_b(r, \theta, z) = v_{b,\theta}(r)\hat{e}_\theta + v_{b,z}(r)\hat{e}_z$$

The self-generated electric field $\mathbf{E_r}(r)$ induced by the space charge, azimuthal self-magnetic field induced by the axial current $\mathbf{J_z}(r)$, and axial self-magnetic field induced by the azimuthal current $\mathbf{J}_\theta(r)$. One can find the self-generated field from the steady state Maxwell equations.

Within above assumptions, the equilibrium self-generated field components are

$$\begin{aligned} \mathbf{E}(r, \theta, z) &= E_r(r)\hat{e}_r \\ \mathbf{B}^s(r, \theta, z) &= B_\theta(r)\hat{e}_\theta + B_z(r)\hat{e}_z \end{aligned} \tag{2}$$

Therefore the self-generated fields are determined from the steady-state Maxwell's equations

$$\nabla \cdot \mathbf{E}(\mathbf{r}) = \frac{1}{r}\frac{\partial}{\partial r}\big(rE_r(r)\big) = 4\pi\rho_0(r)$$

$$\nabla \times \mathbf{B}(\mathbf{r}) = -\frac{\partial B_z(r)}{\partial r}\hat{e}_\theta + \frac{1}{r}\frac{\partial B_\theta(r)}{\partial r}\hat{e}_z \tag{3}$$

$$= \frac{4\pi}{c}\big(J_\theta(r)\hat{e}_\theta + J_z(r)\hat{e}_z\big)$$

where $\rho_0(r) = -ef_b(r)$ is charge density, $J_z(r) = -f_b(r)ev_z$ is axial current density, $J_\theta(r) = -f_b(r)ev_\theta$ is azimuthal current density and $f_b(r)$ is electron beam profile function. The axial velocity and azimuthal velocity of electron beam are $v_z = \beta_b c$ and $v_\theta = r\omega_r$, where $\beta_b = v_b c$ is the normalized axial velocity, ω_r is the angular velocity.

The self-generated field amplitude depends on the electron beam profile. We consider Gaussian shape electron beam. The profile function $f_b(r)$ for the Gaussian density is

$$f_b(r) = \frac{c_n n_b}{\sqrt{2\pi r_b^2}}\exp\left(-\frac{r^2}{2r_b^2}\right) \tag{4}$$

where $c_n = \pi r_b^2$ is the normalized factor and the self electric and magnetic field are

$$\mathbf{E_r^s}(\mathbf{r}) = -\frac{2\alpha r_b^2}{r}\left[1 - \exp\left(-\frac{r^2}{2r_b^2}\right)\right]\hat{e}_r$$

$$\mathbf{B_\theta^s}(\mathbf{r}) = -\frac{2\alpha\beta_b r_b^2}{r}\left[1 - \exp\left(-\frac{r^2}{2r_b^2}\right)\right]\hat{e}_\theta \tag{5}$$

$$\mathbf{B_z^s}(\mathbf{r}) = -\frac{2\alpha\omega_r r_b^2}{c}\left[\exp\left(-\frac{r^2}{2r_b^2}\right) - \exp\left(-\frac{r_w^2}{2r_b^2}\right)\right]\hat{e}_z$$

Figure 1: Cross section views of electrons at (a) the entrance of wiggler and (b) the end of wiggler for $\kappa_s = 2$, a_g=0 and (c) $\kappa_s = 2$, a_g=-2, ϵ_t=0. Dotted(solid) line indicate $r = r_b(2r_b)$.
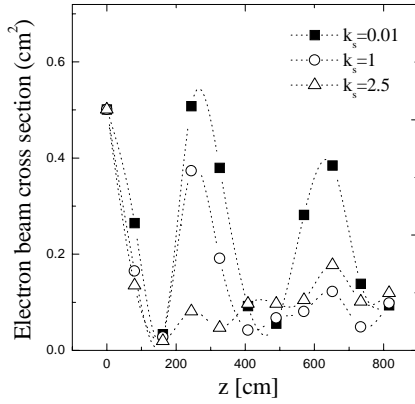
Figure 2: The electron beam cross section along z-axis of the wiggler for various self-field parameters.
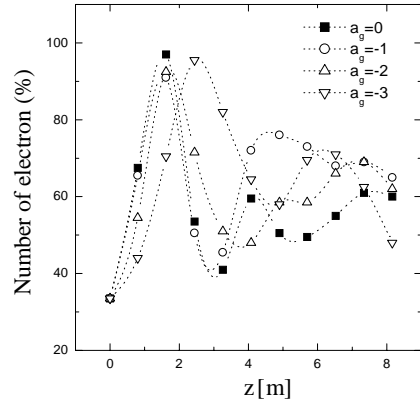
Figure 3: Number of electron along z-axis of the wiggler in r_b for various reversed axial guide field strength.

where $\alpha = \pi e n_b$, $\omega_p = (4\pi n_b e^2/m_e)^{1/2}$ is plasma frequency of electron beam, $\omega_r = k_w c\beta$ is the angular velocity, r_b is the electron beam radius and r_w is the cylindrical waveguide radius.

The scalar potential and vector potential of the self-generated field which satisfies $\mathbf{E_s} = -\nabla \Phi_s$ and $\mathbf{B^s} = \nabla \times \mathbf{A^s}$ are

$$\Phi_s = \alpha r_b^2 \left[\Gamma - \text{Ei}\left(-\frac{r^2}{2r_b^2}\right) - \log\left(\frac{r^2}{2r_b^2}\right) \right]$$

$$\mathbf{A_\theta^s} = \mathbf{\Phi_s}\beta_b \hat{e}_z$$

$$\mathbf{A_z^s} = \frac{\alpha\omega_r r_b^2}{cr} \left[2r_b \exp\left(-\frac{r^2}{2r_b^2}\right) \right.$$
$$\left. + (r^2 + 2r_b^2 - r_w^2)\exp\left(-\frac{r_w^2}{2r_b^2}\right) \right] \hat{e}_\theta \quad (6)$$

where $\text{Ei}(\text{x}) = \int_{-\infty}^{\text{x}} \frac{e^{-u}}{u} du$ is exponential integrate function, and $\Gamma = \lim_{m \to \infty} \left(\sum_{k=1}^{m} \frac{1}{k} - \log m\right) \approx 0.577$ is

Euler-Mascheroni constant.

The vector potential of helical wiggler magnetic field in Cylindrical coordinate system is defined as

$$\mathbf{A_w} = \frac{B_w}{k_w}\left[\left(I_0(k_w r) + I_2(k_w r)\right)\cos(k_w z - \theta)\right]\hat{e}_r$$
$$+ \frac{B_w}{k_w}\left[\left(I_0(k_w r) - I_2(k_w r)\right)\sin(k_w z - \theta)\right]\hat{e}_\theta \quad (7)$$

and vector potential of axial-guide field $\mathbf{B_g} = B_g \hat{e}_z$ which steer the electron to axial direction is $\mathbf{A_g} = \frac{1}{2}B_g r \hat{e}_\theta$.

HAMILTONIAN FORMALISM AND THE TAPERING PROFILE OF GUIDE MAGNETIC FIELD

The Hamiltonian of relativistic test electron is

$$\mathbf{H} = \sqrt{(c\mathbf{P} + e\mathbf{A})^2 + m_e^2 c^4} - e\Phi_s \equiv \gamma m_e c^2 - e\Phi_s \quad (8)$$
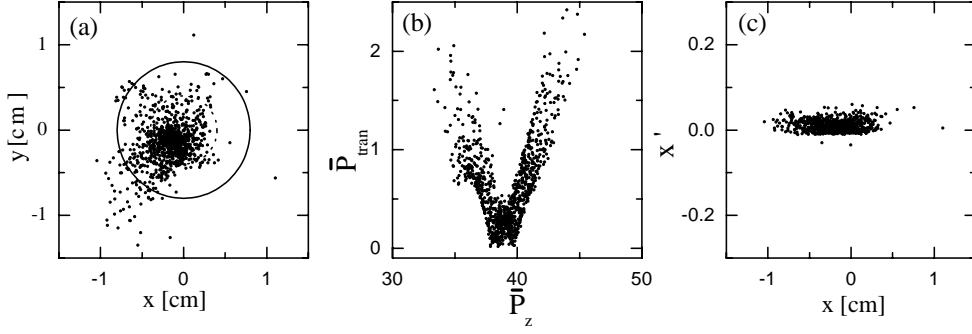
Figure 4: Electron beam profiles at the exit of the wiggler for $a_w = 3$, $\kappa_s = 2$, $a_g = -2$, $\epsilon_t = 0.6$. Dotted(solid) line indicate $r = r_b(2r_b)$.
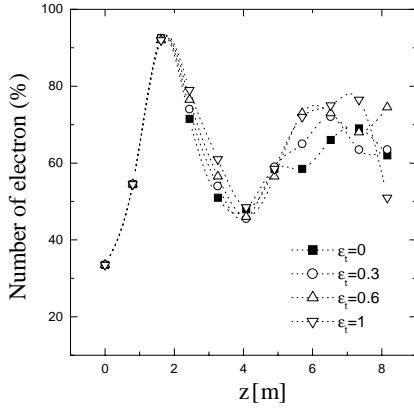
Figure 5: Number of electron along the z-axis of wiggler in r_b for various tapering parameters.

where $\mathbf{P}$ is the canonial momentum, $\mathbf{p} = \mathbf{P} + e\mathbf{A}/c$ is the mechanial momentum, $\gamma = \sqrt{1 + (\mathbf{p}/m_e c)^2}$ is the relativistic mass factor, m_e is the electron rest mass, e is the electron charge and total vector potential is $\mathbf{A} = \mathbf{A_w} + \mathbf{A_g} + \mathbf{A_\theta^s} + \mathbf{A_z^s}$.

Conveniently, we introduce the dimensionless potentials, canonical momentum, and Hamiltonian defined by

$$\bar{\mathbf{A}} = \frac{e\mathbf{A}}{m_e c^2 k_w}, \ \bar{\mathbf{\Phi}}_s = \frac{e\mathbf{\Phi}_s}{m_e c^2 k_w}, \ \bar{\mathbf{P}} = \frac{\mathbf{P}}{m_e c}, \ \bar{\mathbf{H}} = \frac{\mathbf{H}}{m_e c^2} \quad (9)$$

In the dimensionless scalar and vector potential of self-field, the constant α becomes $\alpha = \kappa_s k_w^2/4$, where $\kappa_s = \omega_p^2/c^2 k_w^2$ is the dimensionless strength of the self-field.

Therefore the dimensionless Hamiltonian is

$$\bar{\mathbf{H}} = \sqrt{1 + (\bar{\mathbf{P}} + \bar{\mathbf{A}})^2} - \bar{\mathbf{\Phi}}_s = \sqrt{1 + \Sigma h_i^2} - \bar{\mathbf{\Phi}}_s$$
$$h_1 = \bar{P}_r + a_w(I_0(\bar{r}) - I_2(\bar{r}))\cos(\bar{z} - \theta)$$
$$h_2 = \frac{\bar{P}_\theta}{\bar{r}} + \frac{a_g \bar{r}}{2} + \bar{A}_\theta^s + a_w(I_0(\bar{r}) + I_2(\bar{r}))\sin(\bar{z} - \theta) \quad (10)$$
$$h_3 = \bar{P}_z + \bar{A}_z^s$$

where $a_g = eB_g/m_e c^2 k_w$ is a dimensionless axial-guide field strength, $a_w = eB_w/m_e c^2 k_w$ is a dimensionless wiggler field amplitude, and $\bar{r} = k_w r$, $\bar{z} = k_w z$.

The tapered guide magnetic field $a_g(z) = a_g(0)f_t(z)$, where $f_t(z)$ is the tapering profile function.

$$f_t(z) = \begin{cases} 1 & \text{for } 0 \leq z < z_t \\ 1 + c_n \epsilon_t(z - z_t) & \text{for } z > z_t \end{cases} \quad (11)$$

where z_t is the starting position of the tapering, ϵ_t is tapering parameter, and c_n is constant which satisfy $f_t(z = z_f, \epsilon_t = 1) = 2$. The electron orbits can be calculated from the equation of motions which derived from the Hamiltonian of Eq. 10.

We make the incident electron beam using the beam parameters such as electron beam energy $E_b = 3$ MeV, energy spread $E_s = 5$ %, emittance $\epsilon_{x,y} = 10 \ \pi\text{mm} \cdot \text{mrad}$. Fig. 1(a) shows the cross section view of the incident electron beam which is the initial state of the Gaussian random distribution. Fig. 1(b) shows the cross section views at the exit of the wiggler for self-field parameters $\kappa_s = 2$ without axial guide field, and (c) with uniform axial guide field $a_g = -2$ for $a_w = 3$. Those parameters correspond to the wiggler magnetic field strength $B_w = 2.67$ kG, the guide magnetic field strength $B_w = 1.78$ kG and the electron beam current $I_b = 368$ A for wiggler period $\lambda_w = 12$ cm and electron beam radius $r_b = 0.4$ cm.

Fig. 2 shows the electron beam cross section area along z-axis of the wiggler for various self-field parameter stength. The cross section area is reduced by increasing self-field parameter. Number of electron in r_b along z-axis
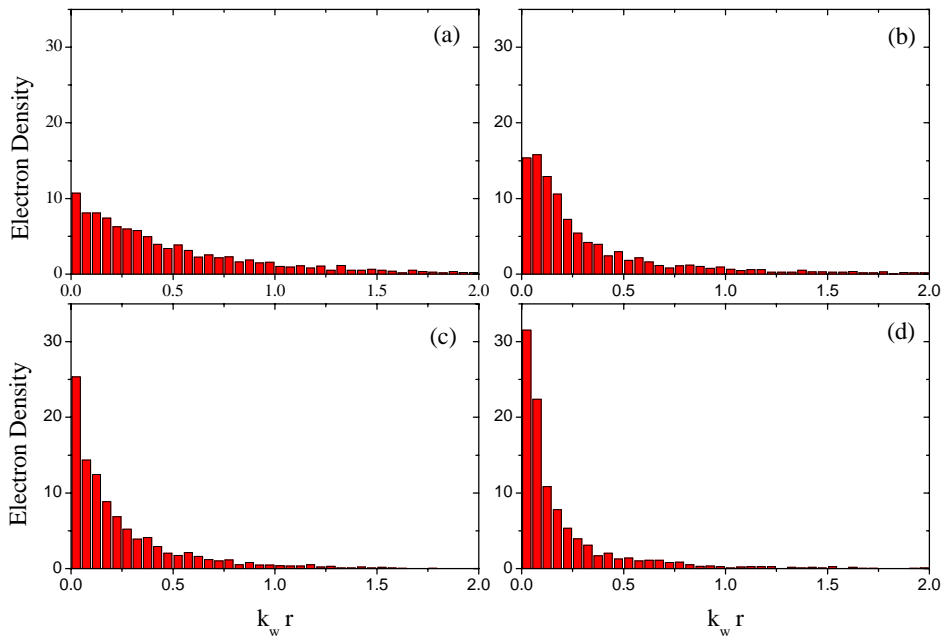
Figure 6: Electron beam density versus $k_w r$; (a) incident electron beam, (b) $\kappa_s = 2$ and $a_g = 0$, (c) $\kappa_s = 2$, $a_g = -2$ and $\epsilon_t = 0$, (d) $\kappa_s = 2$, $a_g = -2$ and $\epsilon_t = 0.6$.

of the wiggler for various reversed axial guide field strength is shown in Fig. 3.

Fig. 4 shows the cross section view, transverse momentum variation and x versus x' phase space for $\kappa_s = 2$, $a_g = -2$ and $\epsilon = 0.6$. The number of electron in r_b along z-axis of the wiggler for various tapering parameters is shown in Fig. 5. The electron densities versus $k_w r$ are shown in Fig. 6. The electron density with tapered and reversed axial guide field is increased by about twice correspond to that of without axial guide field case in center of electron beam.

CONCLUSION

We studied behaviour of electron beam in combined a self-generated field and a reversed axial-guide field in the helical wiggler. Evolution of energy spread and emittance of electron beam were investigated by using three dimensional simulation. Beam cross-section, transverse momentum variation and cross-section view of electron beam were also calculated along z axis. The electron beam loss was reduced by optimizing the magnetic field strength and tapering parameter of reversed axial guide field.

ACKNOWLEDGEMENTS

REFERENCES

[1] L. Friedland, Phys. Fluids. **23** (1980) 2376.

[2] P. Diament, Phys. Rev. **A23** (1981) 2537.

[3] H. P. Freund and A. T. Drobot, Phys. Fluids. **25** (1982) 736.

[4] H. P. Freund, Phys. Rev. **A27** (1983) 1977.

[5] C. Chen and R. C. Davidson, Phys. Fluids. **B2** (1990) 171.

[6] C. Chen and R. C. Davidson, Phys. Rev. **A43** (1991) 5541.

[7] L. Michel, A. Bourdier and J. M. Buzzi, Nucl. Instri. and Meth. **A304** (1991) 465.

[8] S. Spindler and G. Renz, Nucl. Instri. and Meth. **A304** (1991) 492.

[9] L. Michel-Lours, A. Bourdier and J. M. Buzzi, Phys. Fluids. **B5** (1993) 965.

[10] A. Bourdier and L. Michel-Lours, Phys. Rev. **E49** (1994) 49.

[11] R. C. Davidson, *Physics of Nonneutral Plasmas* (Addison Wesley, 1990).